**Article ID**: 1000-7032(2022)05-0763-10

# High-efficiency Blue Phosphorescent OLEDs Based on Mixed-host Structure by Solution-processed Method

WANG Zhe[1,2], WU Rui-xia[1], FENG Yang[1], LIU Hua[2*], ZHOU Liang[1*]

(1. *State Key Laboratory of Rare Earth Resource Utilization, Changchun Institute of Applied Chemistry, Chinese Academy of Sciences, Changchun* 130022, *China*;
2. *Center for Advanced Optoelectronic Functional Materials Research, and Key Laboratory of UV Light-emitting Materials and Technology of Ministry of Education, Northeast Normal University, Changchun* 130024, *China*)

* *Corresponding Authors, E-mail: liuh*146@ *nenu. edu. cn; zhoul@ ciac. ac. cn*

**Abstract**: Blue phosphorescent organic light-emitting diodes (PHOLEDs) which utilized TcTa and CzSi as the mixed-host were fabricated to improve the efficiency by solution-processed method. Additionally, three electron transport materials Tm3PyP26PyB, TmPyPB and TPBi were employed to further enhance the efficiency of devices. The efficiency was improved by optimizing the ratio of host materials and the selection of electron transport material. Finally, the optimal device with the doping ratio TcTa: CzSi of 6∶1 and 70 nm TPBi layer exhibited the maximum brightness ($B_{max}$), current efficiency ($CE_{max}$), power efficiency ($PE_{max}$) and external quantum efficiency ($EQE_{max}$) of 6 662 cd · $m^{-2}$, 39.40 cd · $A^{-1}$, 23.33 lm · $W^{-1}$ and 19.7%, respectively. Moreover, outstanding current efficiency and external quantum efficiency as high as 33.43 cd · $A^{-1}$ and 16.7%, respectively, were obtained, even at the practical brightness of 1 000 cd · $m^{-2}$.

**Key words**: organic light-emitting diodes; high efficiency; solution-processed; mixed-host structure; blue emission
**CLC number**: TN383$^{+}$.1 **Document code**: A **DOI**: 10.37188/CJL.20220049

# 基于混合主体结构的溶液法制备的高效蓝色磷光 OLED

王 哲[1,2], 武瑞霞[1], 冯 洋[1], 刘 华[2*], 周 亮[1*]

(1. 中国科学院长春应用化学研究所 稀土资源利用国家重点实验室, 吉林 长春 130022;
2. 东北师范大学 先进光电子功能材料研究中心, 紫外光发射材料与技术教育部重点实验室, 吉林 长春 130024)

**摘要**: 为了提高蓝色有机发光二极管的效率,本文借助溶液法采用 TcTa 和 CzSi 混合主体,制备了蓝色磷光有机发光二极管(PHOLEDs)。此外,针对三种电子传输材料 Tm3PyP26PyB、TmPyPB 和 TPBi 进行了优选,以进一步优化器件的效率。本文通过优化混合主体材料的掺杂比例和电子传输材料的选择,不断提高器件的效率。最终,当 TcTa: CzSi 的掺杂比为6∶1、电子传输层 TPBi 为 70 nm 时器件性能最优,其最大亮度($B_{max}$)、电流效率($CE_{max}$)、功率效率($PE_{max}$)和外量子效率($EQE_{max}$)分别为 6 662 cd · $m^{-2}$、39.40 cd · $A^{-1}$、23.33 lm · $W^{-1}$和 19.7%。此外,即使在 1 000 cd · $m^{-2}$的实际亮度下,电流效率和外量子效率仍高达 33.43 cd · $A^{-1}$和 16.7%。

**关 键 词**: 有机发光二极管; 高效; 溶液法; 混合主体结构; 蓝光

**收稿日期**: 2022-02-16; **修订日期**: 2022-03-04
**基金项目**: 国家自然科学基金(62174160); 中国科学院科研设备开发项目(YJKYYQ20200005)资助
Supported by National Natural Science Foundation of China(62174160); Research Equipment Development Project of Chinese Academy of Sciences(YJKYYQ20200005)

## 1 Introduction

Organic light-emitting diodes (OLEDs) are the most promising new display and lighting technology owing to their unique advantages of thinness, quick response, high contrast ratio, energy efficiency and being used in flexible electrical appliances[1-3]. It is widely used in smart phone displays, TV screens and computer monitors, *etc*. However, due to the limitation in vacuum thermal evaporation technology, OLEDs have encountered great difficulties in meeting the requirements of low-cost and high-resolution for large-size OLED devices. Therefore, solution-processed OLEDs which have a variety of advantages, such as low fabrication cost, easily scalable manufacturing and the potential in producing large-area devices, have attracted great attention[4]. Conventional OLEDs are typically composed of four or more multiple layers of different materials, thus achieving notable increase in efficiency and lifetime. However, it is more difficult to construct so many layers in the case of solution-processed method, because depositing one layer would dissolve its next layer[5]. Up to now, the blue device still has the issue of low efficiency. In this case, improving the efficiency of blue devices fabricated by solution-processed method becomes more challenging[6].

In recent years, significant improvement has been achieved regarding to solution-processed OLEDs[7-9]. The mixed-host structure has been proposed and its superior advantages in reducing layer structure and improving device performance has been demonstrated. The mixed-host structure used in solution-processed OLEDs is more beneficial for balance the carriers and broaden the recombination zone than the single-host. Chen *et al*. fabricated blue OLEDs using electron-type host material 2, 7-bis (diphenylphosphoyl-9, 9′-spinodimer [fluorene] (SPPO13) and hole-type host material 4,4′,4″-tris (9-carbazolyl) triphenylamine (TcTa)[10]. The luminous efficiency and efficiency roll-off of devices were significantly enhanced and improved by exploiting mixed-host structure than single-host structure. Finally, the optimal device with the doping ratio SPPO13∶TcTa of 6∶3 demonstrated the $CE_{max}$ of 34.3 cd·$A^{-1}$ and $EQE_{max}$ of 15.2%. Kumar *et al*. selected poly(N-vinylcarbazole) (PVK) and 1,3-bis (N-carbazolyl) benzene (mCP) as host materials for efficient red-orange TADF solution-processed OLEDs. The efficiency, lifetime and stability of devices were notable improved by reducing the self-aggregation of TADF emitters. Finally, the optimal device realized the $EQE_{max}$ of 9.75%, $CE_{max}$ of 19.36 cd·$A^{-1}$ and $PE_{max}$ of 12.17 lm·$W^{-1}$ by using the mixed-host structure[11]. In addition, the transmission characteristics of the host materials and the well-matched energy levels between the functional layers are also important factors for the optoelectronic performance of devices.

In this paper, a series of blue phosphorescent devices which utilized iridium (Ⅲ) [bis (4, 6-difuorophenyl) pyridinato-N, C2′] picolinate (FIrpic) as emitter were fabricated to enhance device performances by constructing mixed-host structure consist of TcTa and 9-(4-tert-Butylphenyl)-3,6-bis(triphenylsilyl)-9H-carbazole (CzSi). In addition, the selection of electron transport material was optimized to further improve the efficiency of blue phosphorescent devices. The optimal device displayed the $B_{max}$, $EQE_{max}$, $CE_{max}$ and $PE_{max}$ up to 6 662 cd·$m^{-2}$, 19.7%, 39.40 cd·$A^{-1}$ and 23.33 lm·$W^{-1}$, respectively. Even at the practical brightness of 1 000 cd·$m^{-2}$, current efficiency and external quantum efficiency reach up to 33.43 cd·$A^{-1}$ and 16.7%, respectively, can still be maintained. The high efficiency blue OLEDs with mixed-host structure have been achieved by selecting appropriate host and electron transport material.

## 2 Experiments

All organic materials and solvents were obtained commercially and used as received without further purification. Indium-tin-oxide (ITO) coated glass with a sheet resistance of 10 Ω·$□^{-1}$ was used as the anode. The ITO glass substrates were cleaned with detergent and de-ionized water and finally dried in an oven before preparing the devices. After that, ITO substrates were treated with UV-ozone for 20

min. Poly(3,4-ethylenedioxythiophene): poly(styrene sulfonate) (PEDOT: PSS) was spin-coated on ITO substrates at 3 000 r/min for 60 s and annealed at 120 ℃ for 20 min. Afterward, the samples were moved into the glove box. The luminescent and host materials were dissolved in chlorobenzene solution at 4 mg · mL$^{-1}$ and 10 mg · mL$^{-1}$, respectively. After the solutions of luminescent material and host materials were prepared in proportion, they were dropped on the ITO substrate. The light-emitting layer (EML) was spin-coated at 3 000 r/min for 30 s and annealed at 70 ℃ for 30 min. And then, electron transport layer(ETL) was deposited with the rate of 0.1 nm · s$^{-1}$ under vacuum ($\leqslant 3.0\times10^{-5}$ Pa). LiF and Al were deposited in another vacuum chamber($\leqslant 8.0\times10^{-5}$ Pa) at 0.01 and 1.0 nm · s$^{-1}$, respectively. The current density-voltage-brightness (*J-V-B*) characteristics of devices were measured by using a programmable Keithley source measurement unit(Keithley 2400 and Keithley 2000) with a silicon photodiode. The EL and photoluminescence(PL) spectra were measured by using a calibrated Hitachi F-7000 fluorescence spectrophotometer.

## 3　Results and Discussion

### 3.1　Optimization of Doping Ratio of Host Materials

Fig. 1 shows the energy level diagrams of devices and molecular structures of materials used in these devices. PEDOT: PSS was used as hole injection and transport material. FIrpic was selected as the luminescent material since it is one of the most commonly used blue phosphorescent material. The energy level of host materials should be higher than that of FIrpic ($E_T$ = 2.62 eV) as far as possible to prevent the energy transfer from guest to host[12-13]. In this case, CzSi and TcTa were employed as the host materials. CzSi ($E_T$ = 3.02 eV) has a high triplet energy level, which enables effective energy transfer from host to guest and reduces energy loss during the transfer process. Simultaneously, TcTa has excellent hole transport capability, which can compensate the deficiency of solution-processed devices in hole transport. Therefore, the designed TcTa and CzSi mixed-host structure can effectively balance the charge within the EML. In this part of experiment, 1,3,5-tris(6-(3-(pyridin-3-yl) phenyl) pyridin-2-yl) (Tm3PyP26PyB) was chosen as electron transport material due to its excellent electron transport properties. Moreover, LiF and Al were utilized as electron injection material (EIL) and the cathode, respectively. To determine the optimal doping concentration of FIrpic, a series of devices with structure of ITO/PEDOT: PSS/FIrpic (*x*%): CzSi/Tm3PyP26PyB(60 nm)/LiF(1 nm)/Al(100 nm) were first fabricated and then measured. The 14% doped EML device exhibited $CE_{max}$, $PE_{max}$, $B_{max}$ and $EQE_{max}$ up to 10.26 cd · A$^{-1}$, 4.68 lm · W$^{-1}$, 4 163 cd · m$^{-2}$ and 5.6%, respectively. Subsequently,

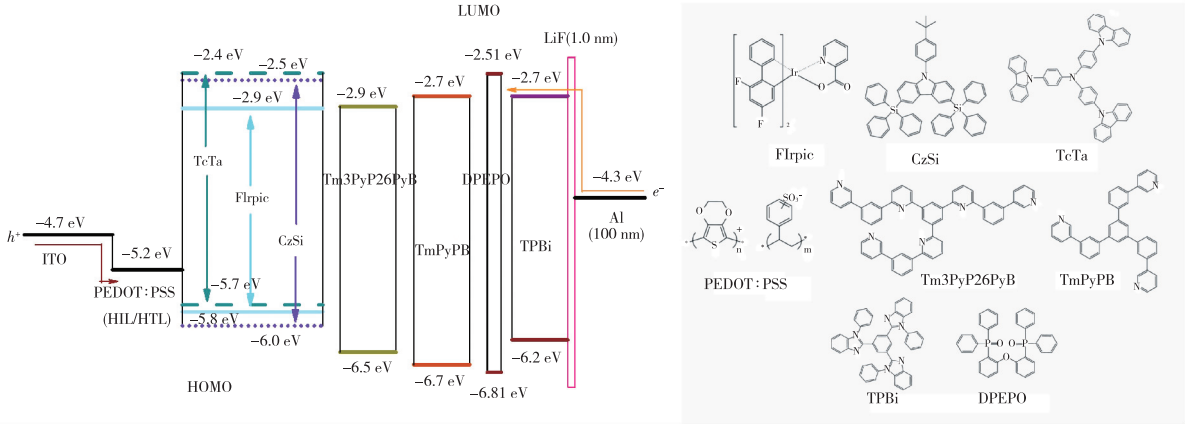


Fig. 1　Energy levels diagram of the devices used in this work and the molecular structures of FIrpic, CzSi, TcTa, PEDOT: PSS, Tm3PyP26PyB, TmPyPB, TPBi and DPEPO.

we introduced TcTa as mixed-host together with CzSi based on the above device architecture to investigate the device performances in mixed-host structure.

Figs. 2(a) – (c) depict current density-voltage-brightness (*J-V-B*) characteristics, the current efficiency-current density ($\eta_c$-*J*) characteristics and current efficiency-brightness-power efficiency ($\eta_c$-*B*-$\eta_p$) characteristics of devices with different doping ratios of TcTa: CzSi, respectively. With the increase in the proportion of TcTa, the current density and current efficiency of devices gradually increased. Moreover, the efficiency of different doping ratios varied little with brightness. Generally, the devices with PEDOT: PSS lack holes within EML due to the large energy gap of hole injection and the high electron mobility of Tm3PyP26PyB, which cause the unbalanced carriers' distribution and the annihilation of excitons. In addition, electrons can transit directly to the guest molecules because of the same lowest unoccupied molecular orbital (LUMO) levels of Tm3PyP26PyB and FIrpic. Obviously, the recombination zone is near the interface between PEDOT: PSS layer and EML. Fig. 2(d) shows the PL spectra and absorption spectra. The peaks of the PL spectra of TcTa, CzSi and TcTa: CzSi were at around 395, 375, 389 nm, respectively. The TcTa: CzSi mixed-host exhibited combined emission of TcTa and CzSi. Therefore, the mixed-host could combine the advantages of the two host materials, which had a good overlap with the absorption spectra of FIrpic, and excitons can transfer from host to FIrpic. Therefore, the hole injection and transport capabilities

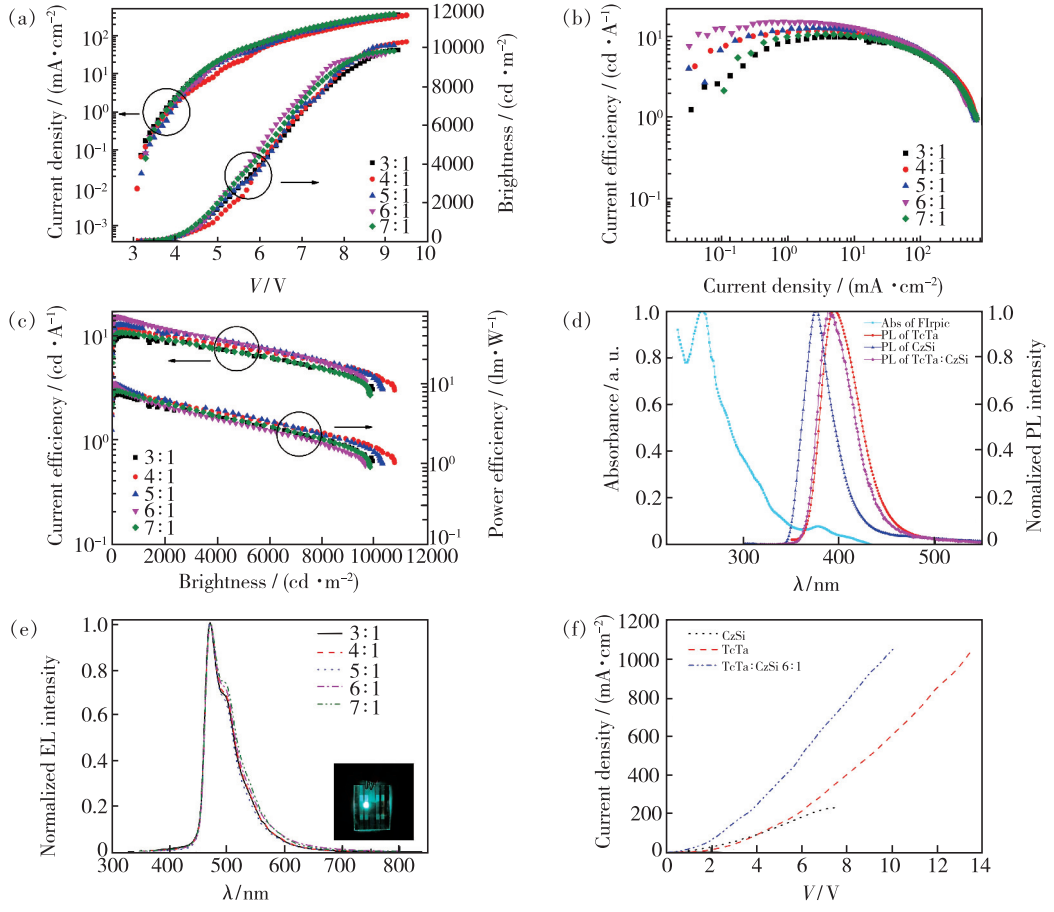


Fig. 2 (a) Current density-voltage-brightness (*J-V-B*) characteristics of devices with different doping ratios of TcTa: CzSi. (b) Current efficiency-current density ($\eta_c$-*J*) characteristics of devices with different doping ratios of TcTa: CzSi. (c) Current efficiency-brightness-power efficiency ($\eta_c$-*B*-$\eta_p$) characteristics of devices with different doping ratios of TcTa: CzSi. (d) Absorption spectra of FIrpic and PL spectra of TcTa, CzSi and TcTa: CzSi. (e) Normalized EL spectra of devices with different doping ratios of TcTa: CzSi operating at 10 mA · $cm^{-2}$. Inset: Photograph of blue OLED. (f) Current density-voltage characteristics of single-hole devices.

of the devices could be improved and the recombination zone should be broadened by increasing the doping ratio of TcTa. When the doping ratio of TcTa: CzSi was 6∶1, the device (device A) achieved the $CE_{max}$, $PE_{max}$, $B_{max}$ and $EQE_{max}$ up to 15.23 cd·A$^{-1}$, 10.32 lm·W$^{-1}$, 9 639 cd·m$^{-2}$ and 7.6%, respectively (see Tab. 1). Consequently, the mixed-host devices exhibit higher performances compared with single-host devices.

**Tab. 1　Key properties of devices with different doping ratios of TcTa: CzSi**

| Device | $V_{turn-on}$/V | $B^a$/(cd·m$^{-2}$) | $\eta_c{}^b$/(cd·A$^{-1}$) (EQE$^c$) | $\eta_p{}^d$/(lm·W$^{-1}$) | $\eta_c{}^e$/(cd·A$^{-1}$) (EQE$^f$) (1 000 cd·m$^{-2}$) | CIE($x$, $y$)$^g$ |
|---|---|---|---|---|---|---|
| 3∶1 | 3.0 | 9 914 | 9.90(5.1%) | 7.45 | 9.67(5.0%) | (0.163, 0.310) |
| 4∶1 | 3.1 | 10 295 | 11.80(6.0%) | 9.08 | 11.01(5.6%) | (0.159, 0.307) |
| 5∶1 | 3.2 | 10 795 | 12.72(6.7%) | 10.05 | 11.83(6.2%) | (0.158, 0.302) |
| 6∶1 | 3.3 | 9 639 | 15.23(7.6%) | 10.32 | 13.43(6.7%) | (0.154, 0.299) |
| 7∶1 | 3.3 | 9 824 | 10.68(5.2%) | 8.22 | 10.24(5.0%) | (0.156, 0.298) |

a The data for maximum brightness($B$), b Maximum current efficiency($\eta_c$), c Maximum external quantum efficiency(EQE), d Maximum power efficiency($\eta_p$), e Current efficiency($\eta_c$) at the certain brightness of 1 000 cd·m$^{-2}$, f External quantum efficiency(EQE) at the certain brightness of 1 000 cd·m$^{-2}$, g Commission Internationale de L'Eclairage coordinates(CIE($x$, $y$)) at 10 mA·cm$^{-2}$.

Meanwhile, the characteristic emission peak and shoulder peak of FIrpic were observed at around 470 nm and 500 nm, respectively, as depicted in Fig. 2(e)[14-16]. Furthermore, the curve progression is very similar and there is no obvious shift in the spectra, which illustrates the stability of the devices. The host emission could not be found in the spectra, indicating that the energy transfer was almost complete between host and guest.

To better illustrate the mixed-host structure enhanced the hole transport ability and thus increased the device efficiency, we fabricated a series of single-hole devices with the structure of ITO/PEDOT: PSS/TcTa/HAT-CN(10 nm)/Al(100 nm), ITO/PEDOT: PSS/CzSi/HAT-CN(10 nm)/Al(100 nm) and ITO/PEDOT: PSS/TcTa: CzSi(6∶1)/HAT-CN(10 nm)/Al(100 nm). As shown in Fig. 2(f), it can be clearly seen that the current density of the mixed-host device was higher than that of the single-host devices. It indicated that the mixed-host structure improved the hole transport ability and made the carriers more balanced, improving device efficiency.

### 3.2　Selection of Electron Transport Material

To further improve the EL performances of FIrpic, we optimized the selection of electron transport material, which is a significant factor besides the doping ratio of host materials. 1,3,5-tri(m-pyrid-3-yl-phenyl)benzene (TmPyPB) and 2,2′,2″-(1,3,5-benzinetriyl)-tris(1-phenyl-1-H-benzimidazole) (TPBi), which have lower electron mobility than that of Tm3PyP26PyB, were selected as the electron transport materials. A series of devices with the structure of ITO/PEDOT: PSS/TcTa: CzSi (6∶1): FIrpic (14%)/TmPyPB ($Y$ nm)/LiF (1 nm)/Al (100 nm) and another series of devices with the structure of ITO/PEDOT: PSS/TcTa: CzSi(6∶1): FIrpic(14%)/DPEPO(10 nm)/TPBi($Z$ nm)/LiF (1 nm)/Al(100 nm) were fabricated and examined by modulating the thickness of the ETL. The electron mobility of TPBi is the lowest among three electron transport materials, which means the slow electrons transport towards EML and causes the shift of recombination zone towards cathode. Therefore, to prevent the transfer of holes into ETL, bis[2-(diphenylphosphino) phenyl] ether oxide (DPEPO) layer was inserted as hole block layer(HBL).

Current density-voltage-brightness and current efficiency-current density characteristics of Tm3PyP26PyB based devices with different ETL thicknesses are depicted in Figs. 3(a) and 3(b). The turn-on voltage increased gradually and the current density decreased gradually with increasing thickness of Tm3PyP26PyB layer. Obviously, increased thickness of ETL can hinder the transportation of

electrons, resulting in increased turn-on voltage and decreased current density. As shown from Fig. 3(c), the roll-off of efficiency tended to slow down with the increasing thickness, but the overall device performance was the best at 60 nm in Tab. 2. Finally, the device with 60 nm ETL(device A) obtained the $CE_{max}$ of 15.23 cd · $A^{-1}$ and $EQE_{max}$ of 7.6%.

**Tab. 2 Key properties of devices with different thicknesses of Tm3PyP26PyB layer**

| Device/ nm | $V_{turn\text{-}on}$/ V | $B^a$/ (cd · $m^{-2}$) | $\eta_c{}^b$/ (cd · $A^{-1}$) (EQE$^c$) | $\eta_p{}^d$/ (lm · $W^{-1}$) | $\eta_c{}^e$/(cd · $A^{-1}$) (EQE$^f$)(1 000 cd · $m^{-2}$) | CIE($x$, $y$)$^g$ |
|---|---|---|---|---|---|---|
| 40 | 2.2 | 7 553 | 6.70(3.7%) | 5.22 | 6.45(3.5%) | (0.153, 0.290) |
| 50 | 3.4 | 8 662 | 10.00(5.3%) | 7.63 | 9.33(5.0%) | (0.153, 0.292) |
| 60 | 3.6 | 9 639 | 15.23(7.6%) | 10.32 | 13.43(6.7%) | (0.154, 0.299) |
| 70 | 3.6 | 10 162 | 13.17(6.7%) | 9.16 | 12.57(6.4%) | (0.149, 0.318) |
| 80 | 4.1 | 6 975 | 11.79(5.9%) | 6.47 | 9.93(5.7%) | (0.154, 0.300) |

a The data for maximum brightness($B$), b Maximum current efficiency($\eta_c$), c Maximum external quantum efficiency(EQE), d Maximum power efficiency($\eta_p$), e Current efficiency($\eta_c$) at the certain brightness of 1 000 cd · $m^{-2}$, f External quantum efficiency(EQE) at the certain brightness of 1 000 cd · $m^{-2}$, g Commission Internationale de L'Eclairage coordinates(CIE($x$, $y$)) at 10 mA · $cm^{-2}$.

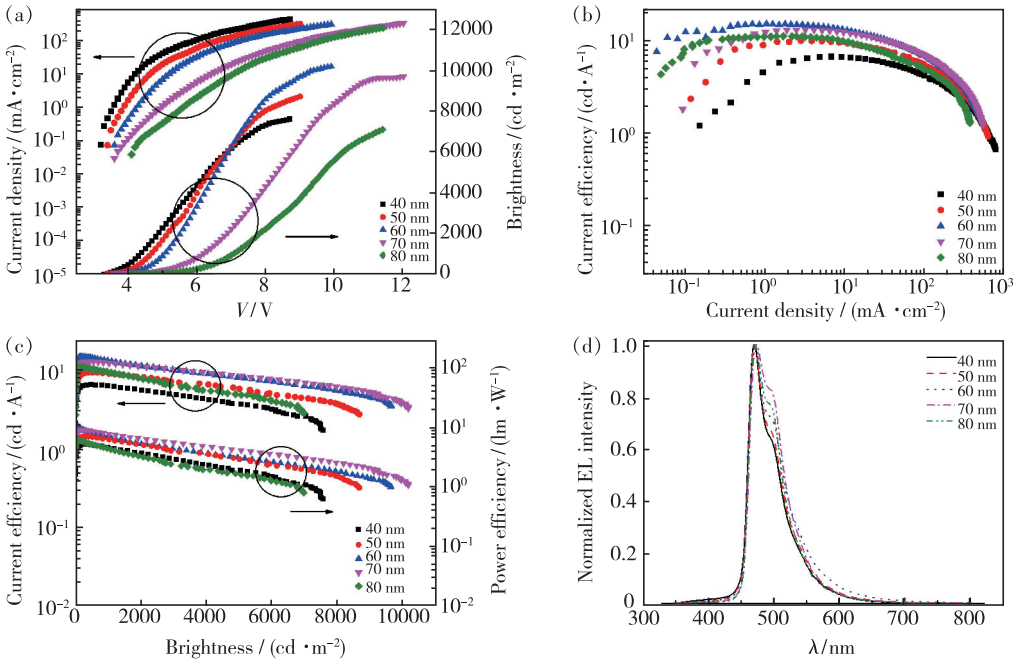


Fig. 3 (a) Current density-voltage-brightness ($J$-$V$-$B$) characteristics of devices with different thicknesses of Tm3PyP26PyB layer. (b) Current efficiency-current density ($\eta_c$-$J$) characteristics of devices with different thicknesses of Tm3PyP26PyB layer. (c) Current efficiency-brightness-power efficiency ($\eta_c$-$B$-$\eta_p$) characteristics of devices with different thicknesses of Tm3PyP26PyB layer. (d) Normalized EL spectra of devices with different thicknesses of Tm3PyP26PyB layer operating at 10 mA · $cm^{-2}$.

Similarly, the same trend was found in TmPyPB and TPBi based devices with different thicknesses of ETL. The characteristics of TmPyPB layer with different thicknesses are shown in Figs. 4(a) – (c). The characteristics of TPBi layer with different thicknesses are shown in Figs. 5(a) – (c). Turn-on voltage and current efficiency increased gradually while current density decreased gradually with increasing thickness of ETL. Finally, the device with 70 nm TmPyPB layer (device B) realized the $CE_{max}$ and $EQE_{max}$ of 28.44 cd · $A^{-1}$ and 14.4%, respectively (see Tab. 3). The device with 70 nm TPBi layer (device C) displayed the $CE_{max}$ and $EQE_{max}$ up to 39.40 cd · $A^{-1}$ and 19.7%, respectively (see Tab. 4).

**Tab. 3　Key properties of devices with TmPyPB layer at different thicknesses**

| Device/ nm | $V_{turn\text{-}on}$/ V | $B^a$/ (cd · m$^{-2}$) | $\eta_c{}^b$/ (cd · A$^{-1}$) (EQE$^c$) | $\eta_p{}^d$/ (lm · W$^{-1}$) | $\eta_c{}^e$/(cd · A$^{-1}$) (EQE$^f$)(1 000 cd · m$^{-2}$) | CIE($x$, $y$)$^g$ |
|---|---|---|---|---|---|---|
| 50 | 3.7 | 8 992 | 21.40(11.9%) | 14.00 | 20.73(11.5%) | (0.149, 0.282) |
| 60 | 4.1 | 8 919 | 25.37(14.2%) | 15.62 | 24.28(13.6%) | (0.148, 0.282) |
| 70 | 3.9 | 9 907 | 28.44(14.4%) | 17.17 | 27.39(13.9%) | (0.150, 0.333) |
| 80 | 4.1 | 7 277 | 27.55(13.0%) | 15.44 | 25.09(11.8%) | (0.157, 0.362) |
| 90 | 5.0 | 4 057 | 30.11(14.8%) | 14.58 | 20.65(10.1%) | (0.154, 0.358) |

a The data for maximum brightness($B$), b Maximum current efficiency($\eta_c$), c Maximum external quantum efficiency(EQE), d Maximum power efficiency($\eta_p$), e Current efficiency($\eta_c$) at the certain brightness of 1 000 cd · m$^{-2}$, f External quantum efficiency(EQE) at the certain brightness of 1 000 cd · m$^{-2}$, g Commission Internationale de L'Eclairage coordinates(CIE($x$, $y$)) at 10 mA · cm$^{-2}$.

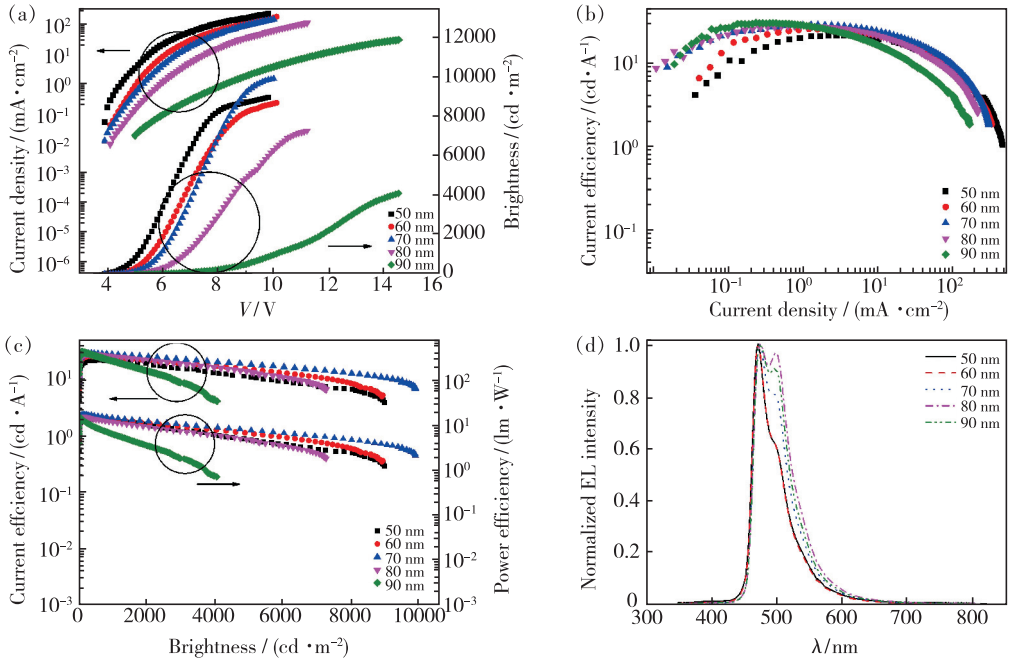


Fig. 4　(a) Current density-voltage-brightness($J$-$V$-$B$) characteristics of devices with TmPyPB layer at different thicknesses. (b) Current efficiency-current density($\eta_c$-$J$) characteristics of devices with TmPyPB layer at different thicknesses. (c) Current efficiency-brightness-power efficiency($\eta_c$-$B$-$\eta_p$) characteristics of devices with TmPyPB layer at different thicknesses. (d) Normalized EL spectra of devices with TmPyPB layer at different thicknesses operating at 10 mA · cm$^{-2}$.

**Tab. 4　Key properties of devices with TPBi layer at different thicknesses**

| Device/ nm | $V_{turn\text{-}on}$/ V | $B^a$/ (cd · m$^{-2}$) | $\eta_c{}^b$/ (cd · A$^{-1}$) (EQE$^c$) | $\eta_p{}^d$/ (lm · W$^{-1}$) | $\eta_c{}^e$/(cd · A$^{-1}$) (EQE$^f$)(1 000 cd · m$^{-2}$) | CIE($x$, $y$)$^g$ |
|---|---|---|---|---|---|---|
| 50 | 4.1 | 6 342 | 33.34(18.6%) | 20.92 | 28.48(15.9%) | (0.148, 0.279) |
| 60 | 4.1 | 5 634 | 39.23(21.4%) | 25.46 | 28.56(15.6%) | (0.147, 0.288) |
| 70 | 4.3 | 6 662 | 39.40(19.7%) | 23.33 | 33.43(16.7%) | (0.146, 0.320) |
| 80 | 4.3 | 5 662 | 36.03(16.4%) | 18.65 | 30.65(14.0%) | (0.155, 0.375) |
| 90 | 4.5 | 5 097 | 35.53(15.2%) | 18.90 | 27.64(11.8%) | (0.169, 0.425) |

a The data for maximum brightness($B$), b Maximum current efficiency($\eta_c$), c Maximum external quantum efficiency(EQE), d Maximum power efficiency($\eta_p$), e Current efficiency($\eta_c$) at the certain brightness of 1 000 cd · m$^{-2}$, f External quantum efficiency(EQE) at the certain brightness of 1 000 cd · m$^{-2}$, g Commission Internationale de L'Eclairage coordinates(CIE($x$, $y$)) at 10 mA · cm$^{-2}$.

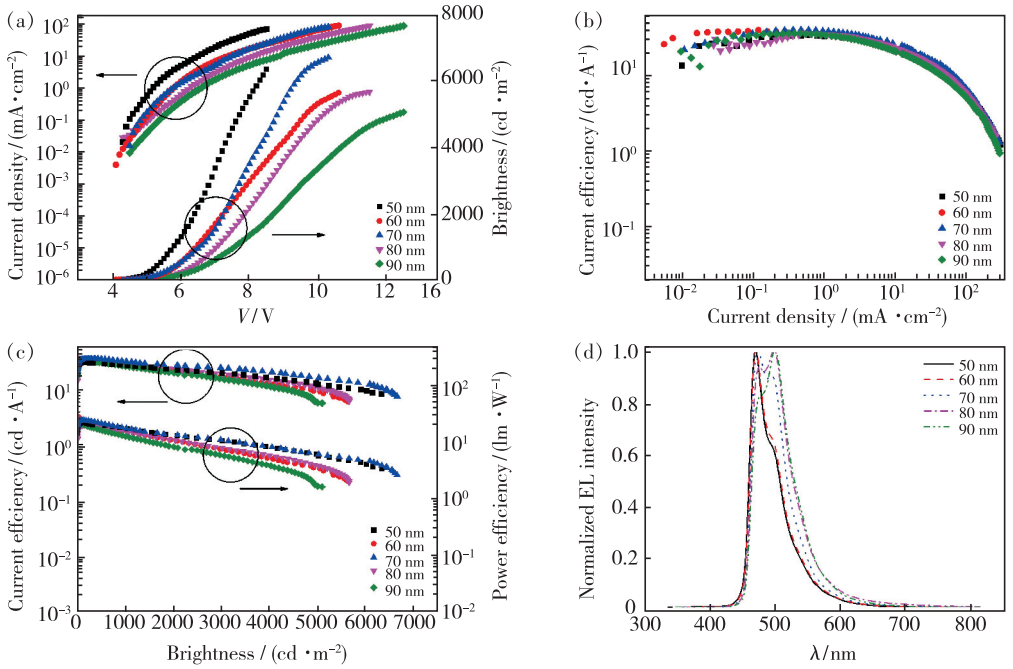


Fig. 5 (a) Current density-voltage-brightness (*J*-*V*-*B*) characteristics of devices with TPBi layer at different thicknesses. (b) Current efficiency-current density ($\eta_c$-*J*) characteristics of devices with TPBi layer at different thicknesses. (c) Current efficiency-brightness-power efficiency ($\eta_c$-*B*-$\eta_p$) characteristics of devices with TPBi layer at different thicknesses. (d) Normalized EL spectra of devices with TPBi layer at different thicknesses operating at 10 mA · cm$^{-2}$.

Figs. 3 (d), 4 (d) and 5 (d) show the EL spectra of devices with Tm3PyP26PyB, TmPyPB and TPBi as ETL, respectively. The emission peak located at 470 nm with a shoulder at 500 nm. The shoulder peaks tended to rise with the increasing thickness of ETL. The shoulder peak at 500 nm is a triplet induced shoulder emission which associated with the characteristic features of FIrpic molecules. The large change in the shoulder peaks is attributed to the weak micro cavity effects raised from the varied optical path of the photons[17]. With the change of ETL thickness, the EL spectra were altered, which may be ascribe to different micro-cavity effect or the changed corresponding metal-to-ligand charge transfer (MLCT) states within FIrpic molecules[18].

Device C showed the highest efficiency among the three devices. Compared with CzSi, the energy barriers of the highest occupied molecular orbital (HOMO) levels of Tm3PyP26PyB, TmPyPB and TPBi were 0.5, 0.7, 0.2 eV, respectively, indicating that device B had the best hole blocking ability. In addition, the triplet energies of Tm3PyP26PyB, TmPyPB and TPBi are 2.8, 2.9, 2.7 eV, respectively, which strongly influence device performances[19-20]. The low triplet energy may reduce the effect of confining triplet state excitons within the EML. However, DPEPO in device C acts as a HBL and has a high triplet energy ($E_T$ = 3.0 eV), which improving the efficiency but also increasing the turn-on voltage. To better understand the mechanisms of performances improvement in these devices, as shown in Fig. 6, the distribution of carriers within the EML of these devices was also analyzed. The experimental results showed that electron mobility has great effect on efficiency of the devices[21]. For these devices, the electron mobility of Tm3PyP26PyB ($2.76\times10^{-4}$ cm$^2$·V$^{-1}$·s$^{-1}$), TmPyPB (~$10^{-5}$ cm$^2$·V$^{-1}$·s$^{-1}$) and TPBi ($5.6\times10^{-8}$ – $2.1\times10^{-5}$ cm$^2$·V$^{-1}$·s$^{-1}$) decreases successively[22-24], meaning decreasing electrons within EML under the same conditions. Luminance of device C was lower than those of devices A and B. However, electrons and holes tended to balance in device C and decreasing electron mobility causes the shift of recombination center towards cathode, thus resulting in widening the recombination zone and suppressing the annihilation of excitons within EML.

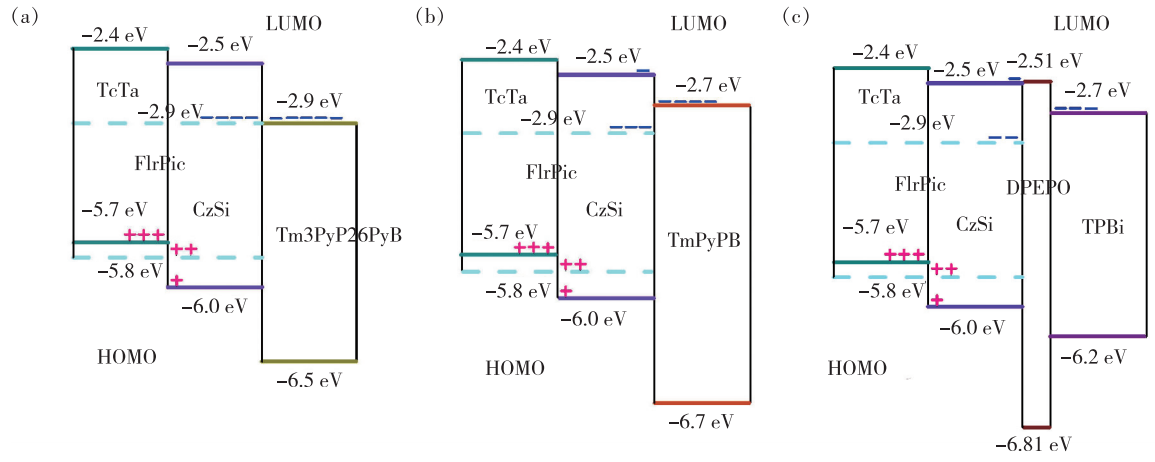


Fig. 6　Carriers' distribution of devices A(a), B(b) and C(c) (Symbols '−' and '+' represent electrons and holes, respectively).

Therefore, device C realized the highest efficiency.

## 4　Conclusion

This work demonstrated that the efficiency of device could be improved by designing mixed-host structure and optimizing the selection of electron transport material. High efficiency blue devices prepared by solution method were achieved by constructing mixed-host structure with the combination of high triplet energy host material with high hole mobility host material. EL efficiency was further improved by selecting a suitable electron transport material. In this case, carriers tended to balance, thus improving device efficiency and reducing exciton quenching. The optimal device with TcTa∶CzSi of 6∶1 and 70 nm TPBi layer displayed the $B_{max}$, $CE_{max}$, $PE_{max}$ and $EQE_{max}$ of 6 662 cd·m$^{-2}$, 39.40 cd·A$^{-1}$, 23.33 lm·W$^{-1}$ and 19.7%, respectively.

Response Letter is available for this paper at: http://cjl.lightpublishing.cn/thesisDetails#10.37188/CJL.20220049.

**References:**

[1] MCCARTHY M A, LIU B, DONOGHUE E P, *et al.* Low-voltage, low-power, organic light-emitting transistors for active matrix displays [J]. *Science*, 2011, 332(6029): 570-573.

[2] GU G, FORREST S R. Design of flat-panel displays based on organic light-emitting devices [J]. *IEEE J. Sel. Top. Quantum Electron*, 1998, 4(1): 83-99.

[3] SHIH C J, LEE C C, YEH T H, *et al.* Versatile exciplex-forming co-host for improving efficiency and lifetime of fluorescent and phosphorescent organic light-emitting diodes [J]. *ACS Appl. Mater. Interfaces*, 2018, 10(28): 24090-24098.

[4] CHO Y R, KIM H S, YU Y J, *et al.* Highly efficient organic light emitting diodes formed by solution processed red emitters with evaporated blue common layer structure [J]. *Sci. Rep.*, 2015, 5: 15903-1-8.

[5] AIZAWA N, PU Y J, WATANABE M, *et al.* Solution-processed multilayer small-molecule light-emitting devices with high-efficiency white-light emission [J]. *Nat. Commun.*, 2014, 5: 5756-1-7.

[6] FAN C, ZHAO F C, GAN P, *et al.* Simple bipolar molecules constructed from biphenyl moieties as host materials for deep-blue phosphorescent organic light-emitting diodes [J]. *Chem. - Eur. J.*, 2012, 18(18): 5510-5514.

[7] SHIN H, LEE J H, MOON C K, *et al.* Sky-blue phosphorescent OLEDs with 34.1% external quantum efficiency using a low refractive index electron transporting layer [J]. *Adv. Mater.*, 2016, 28(24): 4920-4925.

[8] LI Y N, ZHOU L, JIANG Y L, *et al.* High performance pure blue organic fluorescent electroluminescent devices by utilizing a traditional electron transport material as the emitter [J]. *J. Mater. Chem. C*, 2017, 5(17): 4219-4225.

[9] LUCAS F, IBRAIKULOV O A, QUINTON C, *et al.* Spirophenylacridine-2,7-(diphenylphosphineoxide)-fluorene: a bipolar host for high-efficiency single-layer blue phosphorescent organic light-emitting diodes [J]. *Adv. Opt. Mater.*, 2020, 8

(2):1901225-1-8.

[10] CHEN J S,SHI C S,FU Q,*et al*. Solution-processable small molecules as efficient universal bipolar host for blue,green and red phosphorescent inverted OLEDs [J]. *J. Mater. Chem.*, 2012,22(11):5164-5170.

[11] KUMAR M,PEREIRA L. Mixed-host systems with a simple device structure for efficient solution-processed organic light-emitting diodes of a red-orange TADF emitter [J]. *ACS Omega*, 2020,5(5):2196-2204.

[12] HSU F M,CHIEN C H,SHU C F,*et al*. A bipolar host material containing triphenylamine and diphenylphosphoryl-substituted fluorene units for highly efficient blue electrophosphorescence [J]. *Adv. Funct. Mater.*, 2009, 19(17):2834-2843.

[13] GAO C H,MA X J,ZHANG Y,*et al*. 84% efficiency improvement in all-inorganic perovskite light-emitting diodes assisted by a phosphorescent material [J]. *RSC Adv.*, 2018,8(28):15698-15702.

[14] CHIU T L,LEE P Y. Carrier injection and transport in blue phosphorescent organic light-emitting device with oxadiazole host [J]. *Int. J. Mol. Sci.*, 2012,13(6):7575-7585.

[15] WANG J,ZHANG F J,LIU B,*et al*. Emission colour-tunable phosphorescent organic light-emitting diodes based on the self-absorption effect and excimer emission [J]. *J. Phys.* D:*Appl. Phys.*, 2013,46(1):015104-1-9.

[16] LIU J,JIANG M H,ZHOU X Y,*et al*. High-efficient sky-blue and green emissive OLEDs based on FIrpic and FIrdfpic [J]. *Synth. Met.*, 2017,234:111-116.

[17] JESURAJ P J,HAFEEZ H,KIM D H,*et al*. Recombination zone control without sensing layer and the exciton confinement in green phosphorescent OLEDs by excluding interface energy transfer [J]. *J. Phys. Chem.* C, 2018,122(5):2951-2958.

[18] LEE W H,KIM D H,JESURAJ P J,*et al*. Improvement of charge balance,recombination zone confinement,and low efficiency roll-off in green phosphorescent OLEDs by altering electron transport layer thickness [J]. *Mater. Res. Express*, 2018,5(7):076201.

[19] CHEUNG W L,LAI S L,TANG M C,*et al*. High performance gold(ⅲ)-based white organic light-emitting devices with extremely small efficiency roll-off [J]. *J. Mater. Chem.* C, 2019,7(27):8457-8464.

[20] KIM J W,YOO S I,KANG J S,*et al*. Quenching in single emissive white phosphorescent organic light-emitting devices [J]. *Org. Electron.*, 2016,38:230-237.

[21] CHENG G,KUI S C F,ANG W H,*et al*. Structurally robust phosphorescent [Pt(O^N^C^N)] emitters for high performance organic light-emitting devices with power efficiency up to 126 lm · $W^{-1}$ and external quantum efficiency over 20% [J]. *Chem. Sci.*, 2014,5(12):4819-4830.

[22] CUI R Z,LIU W Q,ZHOU L,*et al*. Highly efficient green phosphorescent organic electroluminescent devices with a terbium complex as the sensitizer [J]. *Dyes Pigm.*, 2017,163:361-367.

[23] LI S B,CHEN K,SUN W D,*et al*. High performance yellow phosphorescent organic light-emitting diodes based on an efficient carriers regulating structure with iridium complex as electron manager [J]. *J. Phys. Chem.* C, 2021,125(46):25422-25429.

[24] WANG Y P,LI B,JIANG C,*et al*. Study on electron transport characterization in TPBi thin films and OLED application [J]. *J. Phys. Chem.* C, 2021,125(30):16753-16758.

**王哲**(1997 - ),女,辽宁鞍山人,硕士研究生,2019 年于辽宁师范大学获得学士学位,主要从事有机电致发光二极管制备的研究。

E-mail: 619211510@qq.com

**周亮**(1982 - ),男,江苏徐州人,博士,研究员,博士生导师,2011 年于中国科学院长春应用化学研究所获得博士学位,主要从事有机发光二极管工作机理、有机光电子材料及器件设计、器件制备工艺优化及制备装备的研究。

E-mail: zhoul@ciac.ac.cn

**刘华**(1976 - ),女,吉林长春人,博士,教授,博士生导师,2006 年于中国科学院长春光学精密机械与物理研究所获得博士学位,主要从事衍射光学、非成像光学以及光学设计等领域的研究。

E-mail: liuh146@nenu.edu.cn